

# Weight-adjusted discontinuous Galerkin methods for heterogeneous media and curvilinear meshes

Jesse Chan<sup>1</sup>, Russell Hewett<sup>2</sup>, T. Warburton<sup>3</sup>

<sup>1</sup>Department of Computational and Applied Math, Rice University

<sup>2</sup>TOTAL E&P Research and Technology USA

<sup>3</sup>Department of Mathematics, Virginia Tech

SIAM CSE  
February 28, 2017

# High order DG methods for wave propagation

- Unstructured (tetrahedral) meshes for geometric flexibility.
- Low numerical dissipation and dispersion.
- High order approximations: more accurate per unknown.
- High performance on many-core (explicit time stepping).

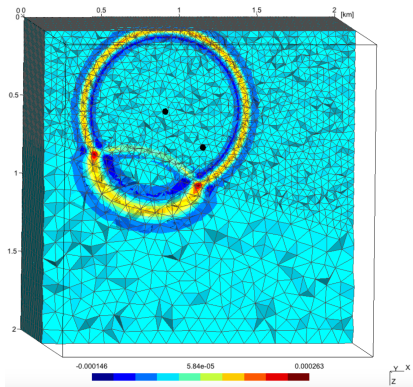
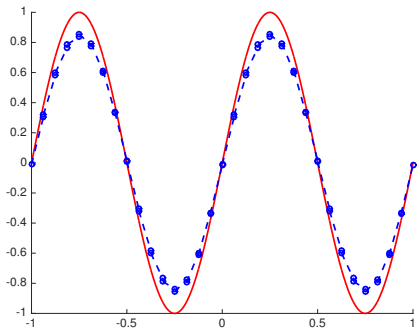


Figure courtesy of Axel Modave.

# High order DG methods for wave propagation

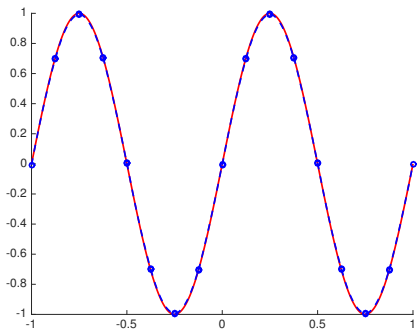
- Unstructured (tetrahedral) meshes for geometric flexibility.
- Low numerical dissipation and dispersion.
- High order approximations: more accurate per unknown.
- High performance on many-core (explicit time stepping).



**Fine** linear approximation.

# High order DG methods for wave propagation

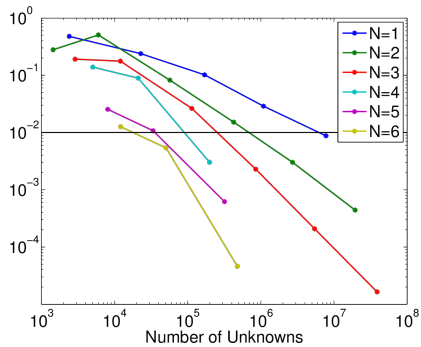
- Unstructured (tetrahedral) meshes for geometric flexibility.
- Low numerical dissipation and dispersion.
- High order approximations: more accurate per unknown.
- High performance on many-core (explicit time stepping).



**Coarse quadratic approximation.**

# High order DG methods for wave propagation

- Unstructured (tetrahedral) meshes for geometric flexibility.
- Low numerical dissipation and dispersion.
- High order approximations: more accurate per unknown.
- High performance on many-core (explicit time stepping).



Max errors vs. dofs.

# High order DG methods for wave propagation

- Unstructured (tetrahedral) meshes for geometric flexibility.
- Low numerical dissipation and dispersion.
- High order approximations: more accurate per unknown.
- High performance on many-core (explicit time stepping).



A graphics processing unit (GPU).

# Energy stable discontinuous Galerkin formulations

- Model problem: acoustic wave equation

$$\frac{1}{c^2} \frac{\partial p}{\partial t} = \nabla \cdot \mathbf{u}, \quad \frac{\partial \mathbf{u}}{\partial t} = \nabla p$$

- (Local) formulation with penalty fluxes

$$\begin{aligned} \int_{D^k} \frac{1}{c^2} \frac{\partial p}{\partial t} q &= \int_{D^k} \nabla \cdot \mathbf{u} q + \frac{1}{2} \int_{\partial D^k} ([\![\mathbf{u}]\!] \cdot \mathbf{n} + \tau_p [\![p]\!]) q \\ \int_{D^k} \frac{\partial \mathbf{u}}{\partial t} \mathbf{v} &= \int_{D^k} \nabla p \cdot \mathbf{v} + \frac{1}{2} \int_{\partial D^k} ([\![p]\!] + \tau_u [\![\mathbf{u}]\!] \cdot \mathbf{n}) \mathbf{v} \end{aligned}$$

- High order accuracy, semi-discrete energy stability

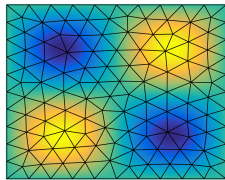
$$\frac{\partial}{\partial t} \left( \sum_k \int_{D^k} \frac{p^2}{c^2} + |\mathbf{u}|^2 \right) = - \int_{\partial D^k} \tau_p [\![p]\!]^2 + \tau_u [\![\mathbf{u} \cdot \mathbf{n}]\!]^2 \leq 0.$$

# High order approximation of media and geometry

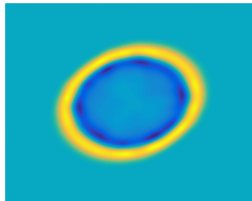
- Efficient implementation on **simplicial** meshes:  $c^2$  piecewise constant, non-curved meshes ( $J, J^f$  piecewise constant).

$$\int_{D^k} \frac{1}{c^2} \frac{\partial p}{\partial t} q = \int_{D^k} \nabla \cdot \mathbf{u} q + \frac{1}{2} \int_{\partial D^k} (\llbracket \mathbf{u} \rrbracket \cdot \mathbf{n} + \tau_p \llbracket p \rrbracket) q$$
$$\int_{D^k} \frac{\partial \mathbf{u}}{\partial t} \mathbf{v} = \int_{D^k} \nabla p \cdot \mathbf{v} + \frac{1}{2} \int_{\partial D^k} (\llbracket p \rrbracket + \tau_u \llbracket \mathbf{u} \rrbracket \cdot \mathbf{n}) \mathbf{v}$$

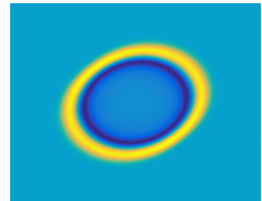
- Spurious reflections for low order approximations of media, geometry.



(a) Mesh and exact  $c^2$



(b) Piecewise const.  $c^2$



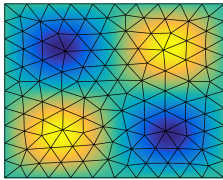
(c) High order  $c^2$

# High order approximation of media and geometry

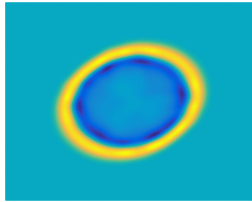
- Efficient implementation on **simplicial** meshes:  $c^2$  piecewise constant, non-curved meshes ( $J, J^f$  piecewise constant).

$$\int_{\hat{D}} \frac{1}{c^2} \frac{\partial p}{\partial t} q J = \int_{\hat{D}} \nabla \cdot \mathbf{u} q J + \frac{1}{2} \int_{\partial \hat{D}} ([\![\mathbf{u}]\!] \cdot \mathbf{n} + \tau_p [\![p]\!]) q J^f$$
$$\int_{\hat{D}} \frac{\partial \mathbf{u}}{\partial t} \mathbf{v} J = \int_{\hat{D}} \nabla p \cdot \mathbf{v} J + \frac{1}{2} \int_{\partial \hat{D}} ([\![p]\!] + \tau_u [\![\mathbf{u}]\!] \cdot \mathbf{n}) \mathbf{v} J^f$$

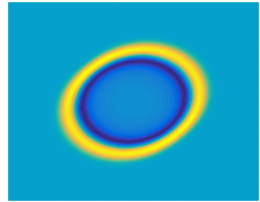
- Spurious reflections for low order approximations of media, geometry.



(a) Mesh and exact  $c^2$



(b) Piecewise const.  $c^2$



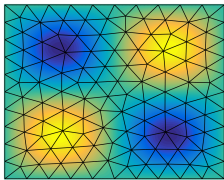
(c) High order  $c^2$

# High order approximation of media and geometry

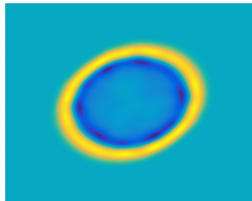
- Efficient implementation on **simplicial** meshes:  $c^2$  piecewise constant, non-curved meshes ( $J, J^f$  piecewise constant).

$$\frac{J}{c^2} \int_{\hat{D}} \frac{\partial p}{\partial t} q = J \int_{\hat{D}} \nabla \cdot \mathbf{u} q + J^f \frac{1}{2} \int_{\partial \hat{D}} ([\![\mathbf{u}]\!] \cdot \mathbf{n} + \tau_p [\![p]\!]) q$$
$$J \int_{\hat{D}} \frac{\partial \mathbf{u}}{\partial t} \mathbf{v} = J \int_{\hat{D}} \nabla p \cdot \mathbf{v} + J^f \frac{1}{2} \int_{\partial \hat{D}} ([\![p]\!] + \tau_u [\![\mathbf{u}]\!] \cdot \mathbf{n}) \mathbf{v}$$

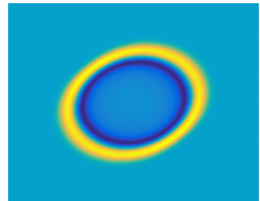
- Spurious reflections for low order approximations of media, geometry.



(a) Mesh and exact  $c^2$



(b) Piecewise const.  $c^2$



(c) High order  $c^2$

# Outline

# Outline

# Weighted mass matrices

- Spatially varying weights appear in DG mass matrices

$$\int_{\hat{D}} \frac{1}{c^2} \frac{\partial p}{\partial t} q J = \text{pressure RHS}, \quad \int_{\hat{D}} \frac{\partial \mathbf{u}}{\partial t} \mathbf{v} J = \text{velocity RHS}$$

- Curvilinear meshes and wave propagation in heterogeneous media

$$(\mathbf{M}_w)_{ij} = \int_{\hat{D}} \phi_i \phi_j w(x),$$

$$\frac{d}{dt} \mathbf{M}_w \mathbf{u} = \text{right hand side.}$$

- Inherits **high order accuracy** and **energy stability** with respect to a weighted  $L^2$  norm, but requires  $\mathbf{M}_w^{-1}$  explicitly over each element.
- On-the-fly assembly + inversion or pre-computation and **storage**.

# Weighted mass matrices

- Spatially varying weights appear in DG mass matrices

$$\int_{\hat{D}} \frac{1}{c^2} \frac{\partial p}{\partial t} q \mathbf{J} = \text{pressure RHS}, \quad \int_{\hat{D}} \frac{\partial \mathbf{u}}{\partial t} \mathbf{v} \mathbf{J} = \text{velocity RHS}$$

- Curvilinear meshes and wave propagation in heterogeneous media

$$(\mathbf{M}_w)_{ij} = \int_{\hat{D}} \phi_i \phi_j \mathbf{J}(\mathbf{x}),$$

$$\frac{d}{dt} \mathbf{M}_w \mathbf{u} = \text{right hand side.}$$

- Inherits **high order accuracy** and **energy stability** with respect to a weighted  $L^2$  norm, but requires  $\mathbf{M}_w^{-1}$  explicitly over each element.
- On-the-fly assembly + inversion or pre-computation and **storage**.

# Weighted mass matrices

- Spatially varying weights appear in DG mass matrices

$$\int_{\hat{D}} \frac{1}{c^2} \frac{\partial p}{\partial t} q J = \text{pressure RHS}, \quad \int_{\hat{D}} \frac{\partial \mathbf{u}}{\partial t} \mathbf{v} J = \text{velocity RHS}$$

- Curvilinear meshes and wave propagation in heterogeneous media

$$(\mathbf{M}_w)_{ij} = \int_{\hat{D}} \phi_i \phi_j \frac{J}{c^2(x)},$$

$$\frac{d}{dt} \mathbf{M}_{J/c^2} \mathbf{u} = \text{right hand side.}$$

- Inherits **high order accuracy** and **energy stability** with respect to a weighted  $L^2$  norm, but requires  $\mathbf{M}_w^{-1}$  explicitly over each element.
- On-the-fly assembly + inversion or pre-computation and **storage**.

# Weighted mass matrices

- Spatially varying weights appear in DG mass matrices

$$\int_{\hat{D}} \frac{1}{c^2} \frac{\partial p}{\partial t} q J = \text{pressure RHS}, \quad \int_{\hat{D}} \frac{\partial \mathbf{u}}{\partial t} \mathbf{v} J = \text{velocity RHS}$$

- Curvilinear meshes and wave propagation in heterogeneous media

$$(\mathbf{M}_w)_{ij} = \int_{\hat{D}} \phi_i \phi_j w(x),$$

$$\frac{d}{dt} \mathbf{M}_w \mathbf{u} = \text{right hand side.}$$

- Inherits **high order accuracy** and **energy stability** with respect to a weighted  $L^2$  norm, but requires  $\mathbf{M}_w^{-1}$  explicitly **over each element**.
- On-the-fly assembly + inversion or pre-computation and **storage**.

# Weight-adjusted DG: convergence and implementation

- Weight-adjusted DG (WADG): energy stable approximation of weighted mass matrix

$$\mathbf{M}_w \frac{d\mathbf{U}}{dt} \approx \mathbf{M} (\mathbf{M}_{1/w})^{-1} \mathbf{M} \frac{d\mathbf{U}}{dt} = \text{right hand side.}$$

- WADG *a-priori* estimates: standard DG  $O(h^{N+1/2})$  convergence of  $L^2$  error based on optimal weighted projection estimate:

$$\|u - P_w u\|_{L^2} \leq Ch^{N+1} \|w\|_{W^{N+1,\infty}} \left\| \frac{\sqrt{J}}{w} \right\|_{L^\infty} \|u\|_{W^{N+1,2}}.$$

- Bypasses inverse of weighted matrix  $(\mathbf{M}_w)^{-1}$

$$(\mathbf{M} (\mathbf{M}_{1/w})^{-1} \mathbf{M})^{-1} = \mathbf{M}^{-1} \mathbf{M}_{1/w} \mathbf{M}^{-1}.$$

# A non-intrusive and low-storage implementation

- Operator evaluation reuses implementation for  $w = 1$

$$\begin{aligned} \mathbf{M} (\mathbf{M}_{1/w})^{-1} \mathbf{M} \frac{d\mathbf{U}}{dt} &= \mathbf{A}_h \mathbf{U} \\ \rightarrow (\mathbf{M}_{1/w})^{-1} \mathbf{M} \frac{d\mathbf{U}}{dt} &= \underbrace{\mathbf{M}^{-1} \mathbf{A}_h \mathbf{U}}_{\text{RHS for } w=1} \end{aligned}$$

- Low storage: matrix-free application of  $\mathbf{M}^{-1} \mathbf{M}_{1/w}$ .

$$(\mathbf{M})^{-1} \mathbf{M}_{1/w} \text{RHS} = \underbrace{\widehat{\mathbf{M}}^{-1} \mathbf{V}_q^T W \text{diag}(1/w) \mathbf{V}_q}_{P_q} (\text{RHS}).$$

- Non-intrusive: modify RHS locally before update. For non-curved meshes, can combine with *optimal complexity* RHS evaluation.<sup>1</sup>

# Weight-adjusted DG: not locally conservative

- **Con:** loss of local conservation for  $w(x) \notin P^N$ !

- **Pro:** superconvergence of conservation error

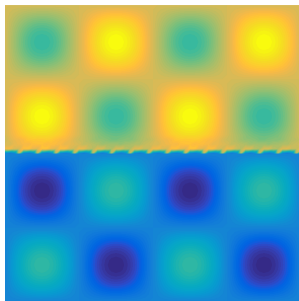
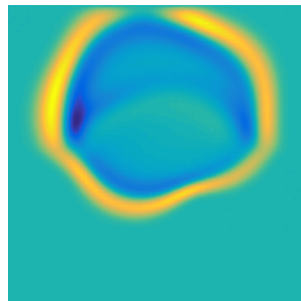
$$\text{Conservation error} \leq Ch^{2N+2} \|w\|_{W^{N+1,\infty}} \|p\|_{W^{N+1,2}}$$

where  $C$  depends on mesh quality and max/min values of  $w$ .

- **Pro:** can restore local conservation with rank-1 update (Shermann-Morrison).

# Outline

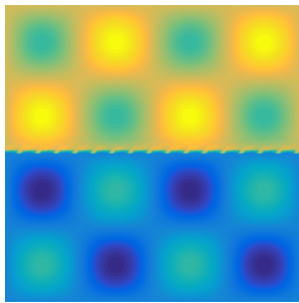
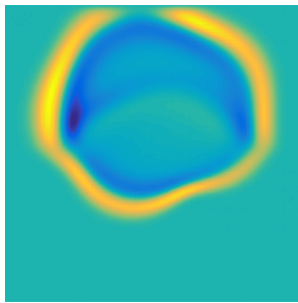
# Acoustic wave equation: variable coefficients

(a)  $c^2(x, y)$ 

(b) Standard DG

Figure: Standard vs. weight-adjusted DG with spatially varying  $c^2$  containing both smooth variations and a discontinuity.

# Acoustic wave equation: variable coefficients

(a)  $c^2(x, y)$ 

(b) Weighted-adjusted DG

Figure: Standard vs. weight-adjusted DG with spatially varying  $c^2$  containing both smooth variations and a discontinuity.

Acoustics, variable coefficients:  $L^2$  errors

Smooth wavefield  $c^2(x, y) = 1 + \frac{1}{2} \sin(\pi x) \sin(\pi y)$

	$h = 1$	$h = 1/2$	$h = 1/4$	$h = 1/8$
DG $N = 1$	2.13e-01	6.25e-02	1.64e-02	4.19e-03
WADG $N = 1$	2.05e-01	5.99e-02	1.62e-02	4.18e-03
DG $N = 2$	3.01e-02	3.60e-03	4.21e-04	5.07e-05
WADG $N = 2$	2.89e-02	3.54e-03	4.18e-04	5.07e-05
DG $N = 3$	6.10e-03	3.33e-04	2.04e-05	1.22e-06
WADG $N = 3$	8.69e-03	3.47e-04	2.03e-05	1.22e-06
DG $N = 4$	6.61e-04	2.12e-05	6.39e-07	1.94e-08
WADG $N = 4$	1.09e-03	2.27e-05	6.30e-07	1.93e-08

Table: Convergence of standard, weight-adjusted DG to a manufactured solution.

Acoustics, variable coefficients:  $L^2$  errors

Smooth wavefield  $c^2(x, y) = 1 + \frac{1}{2} \sin(\pi x) \sin(\pi y)$

	$h = 1$	$h = 1/2$	$h = 1/4$	$h = 1/8$
DG $N = 1$	2.48e-01	7.58e-02	1.69e-02	4.46e-03
WADG $N = 1$	2.50e-01	7.72e-02	1.69e-02	4.47e-03
DG $N = 2$	5.95e-02	9.95e-03	1.10e-03	1.22e-04
WADG $N = 2$	6.09e-02	1.02e-02	1.10e-03	1.22e-04
DG $N = 3$	2.29e-02	1.98e-03	9.52e-05	6.56e-06
WADG $N = 3$	1.98e-02	1.98e-03	9.52e-05	6.56e-06
DG $N = 4$	4.90e-03	3.01e-04	1.78e-05	7.27e-07
WADG $N = 4$	4.64e-03	3.02e-04	1.78e-05	7.28e-07

Table: Convergence to a reference solution ( $N = 100$  spectral method).

# Acoustics, variable coefficients: convergence

	$N = 1$	$N = 2$	$N = 3$	$N = 4$
DG	1.9220	3.0752	4.0440	5.0446
WADG	1.9211	3.0629	4.0752	5.0990

(a) Rates of convergence to manufactured solution

	$N = 1$	$N = 2$	$N = 3$	$N = 4$
DG	1.8256	3.1796	3.8589	4.6171
WADG	1.8425	3.1807	3.8583	4.6128

(b) Rates of convergence to reference solution

Observed  $L^2$  rates between optimal  $O(h^{N+1})$  and estimated  $O(h^{N+1/2})$ .

# Outline

# Weight-adjusted DG for curvilinear meshes

- Weight-adjusted  $L^2$  projection  $\tilde{P}_N$  on curved domains

$$\tilde{P}_N(u) := P_N \left( \frac{1}{J} P_N(uJ) \right).$$

where  $P_N$  is the  $L^2$  projection onto the reference element.

- $L^2$  estimates for weight-adjusted projection:

$$\|u - \tilde{P}_N u\|_{L^2(D^k)} \lesssim \left\| \frac{1}{\sqrt{J}} \right\|_{L^\infty}^2 \|J\|_{W^{N+1,\infty}(D^k)} h^{N+1} \|u\|_{W^{N+1,2}(D^k)}.$$

- High order Sobolev norm of  $J$  - implies that convergence can suffer if mapping is not sufficiently regular.

# Behavior of weight-adjusted $L^2$ projection

Comparison with  $L^2$  projection and Low-Storage Curvilinear DG

$$\tilde{\phi}_i = \frac{\phi_i}{\sqrt{J}}, \quad \mathbf{M}_{ij} = \int_{D^k} \tilde{\phi}_j \tilde{\phi}_i J = \int_{\hat{D}} \phi_j \phi_i = \widehat{\mathbf{M}}_{ij}.$$

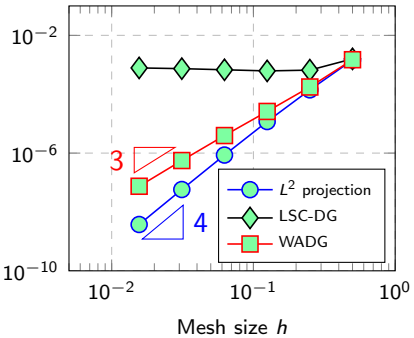
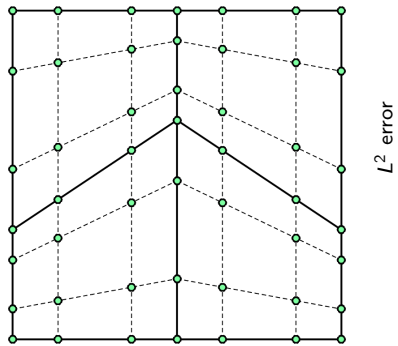


Figure: Arnold-type mesh with  $\|J\|_{W^{N+1,\infty}} = O(h^{-1})$  for  $N = 3$ .

# Behavior of weight-adjusted $L^2$ projection

Comparison with  $L^2$  projection and Low-Storage Curvilinear DG

$$\tilde{\phi}_i = \frac{\phi_i}{\sqrt{J}}, \quad \mathbf{M}_{ij} = \int_{D^k} \tilde{\phi}_j \tilde{\phi}_i J = \int_{\hat{D}} \phi_j \phi_i = \widehat{\mathbf{M}}_{ij}.$$

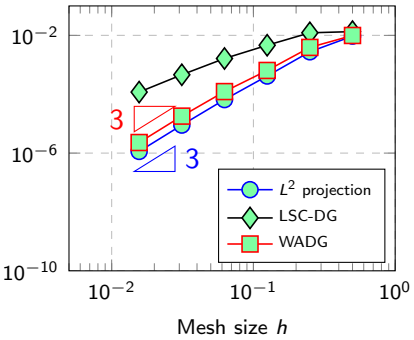
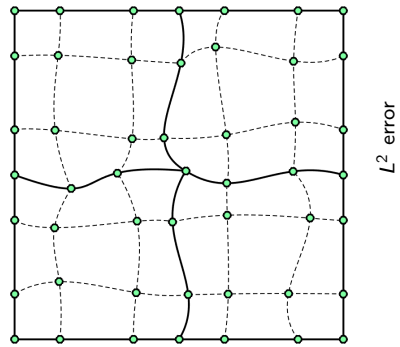


Figure: Curvilinear mesh constructed through random perturbation for  $N = 3$ .

# Behavior of weight-adjusted $L^2$ projection

High order convergence **slowed** by growth of  $\|J\|_{W^{N+1,\infty}} = O(h^N)$ .

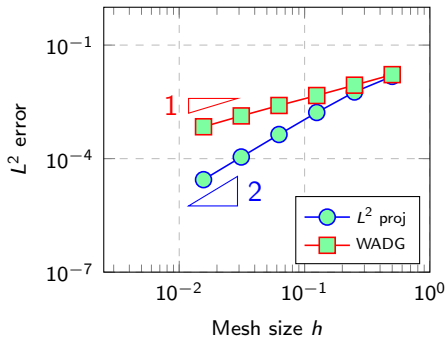
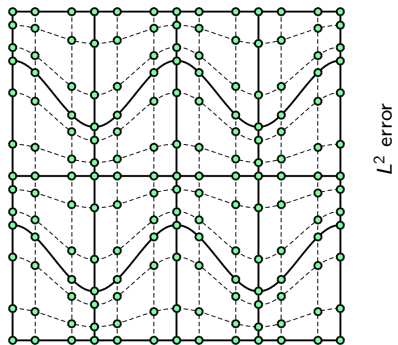


Figure: Moderately warped curved Arnold-type mesh for  $N = 3$ .

# Behavior of weight-adjusted $L^2$ projection

High order convergence is **stalled** by growth of  $\|J\|_{W^{N+1,\infty}} = O(h^{N+1})$ .

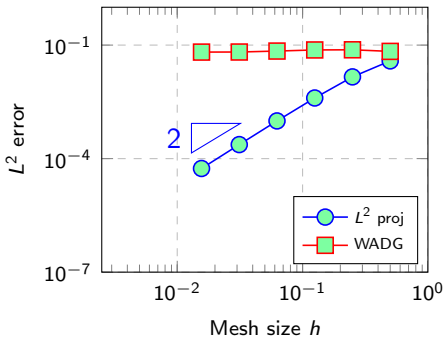
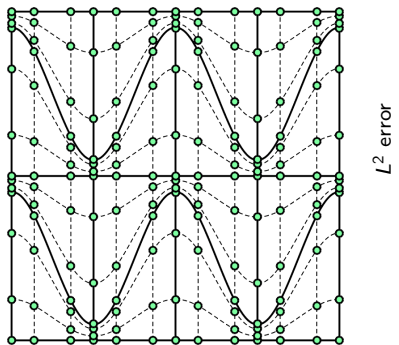


Figure: Heavily warped curved Arnold-type mesh for  $N = 3$ .

# Curvilinear meshes: verification

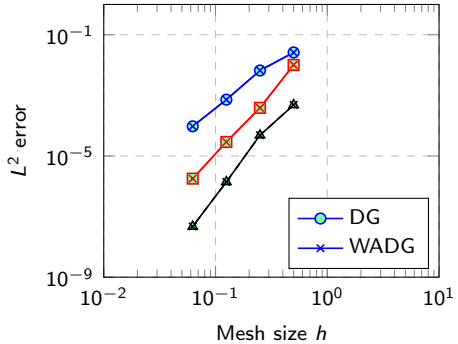
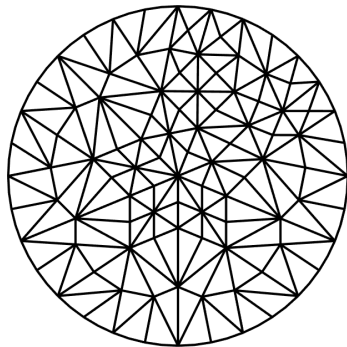
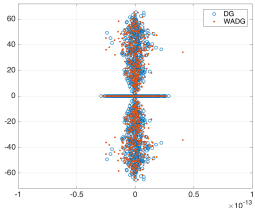
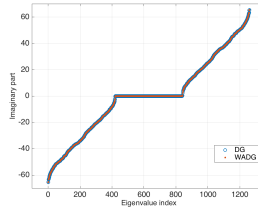
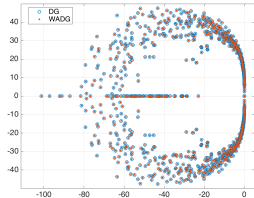
(a)  $L^2$  errors for  $N = 2, 3, 4$ 

Figure: Optimal  $L^2$  convergence rates observed for curvilinear meshes.

# Curvilinear meshes: DG eigenvalues (circular domain)



(a) Central fluxes

(b)  $\text{Im}(\lambda_i)$  for central fluxes

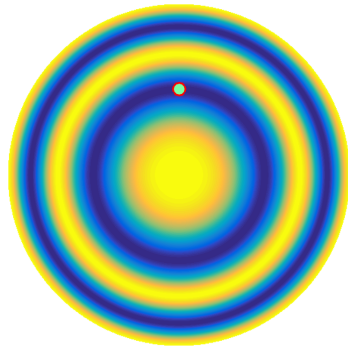
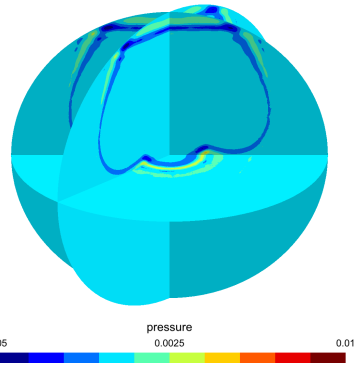
(c) Upwind fluxes

- Energy stability requires quadrature, skew-symmetric formulation

$$\int_{D^k} \frac{\partial p}{\partial t} q = \int_{D^k} -\mathbf{u} \cdot \nabla q + \frac{1}{2} \int_{\partial D^k} (2 \{\{\mathbf{u}\}\} \cdot \mathbf{n} + \tau_p [\![p]\!]) q$$

$$\int_{D^k} \frac{\partial \mathbf{u}}{\partial t} \mathbf{v} = \int_{D^k} \nabla p \cdot \mathbf{v} + \frac{1}{2} \int_{\partial D^k} ([\![p]\!] + \tau_u [\![\mathbf{u}]\!] \cdot \mathbf{n}) \mathbf{v}$$

# Curved meshes + heterogeneous media

(a) Wavespeed  $c^2(x)$ (b) Pressure isovalues at  $t = .6$ 

Straightforward to combine curved elements and heterogeneous media without compromising efficiency.

# Outline

# Matrix-valued weights and elastic wave propagation

- Symmetric velocity-stress form of linear elasticity ( $\mathbf{A}_i$  constant)

$$\rho \frac{\partial \mathbf{v}}{\partial t} = \sum_{i=1}^d \mathbf{A}_i^T \frac{\partial \boldsymbol{\sigma}}{\partial \mathbf{x}_i}, \quad \mathbf{C}^{-1} \frac{\partial \boldsymbol{\sigma}}{\partial t} = \sum_{i=1}^d \mathbf{A}_i \frac{\partial \mathbf{v}}{\partial \mathbf{x}_i}.$$

- DG formulation based on penalty fluxes, matrix-weighted mass matrix

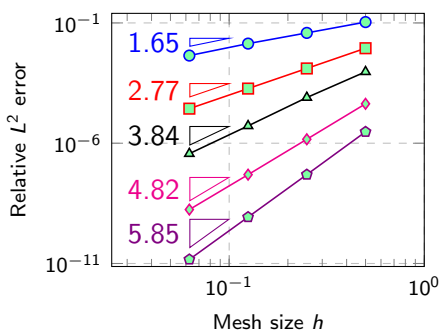
$$(\mathbf{M}_{\mathbf{C}^{-1}})^{-1} = \begin{pmatrix} \mathbf{M}_{C_{11}^{-1}} & \dots & \mathbf{M}_{C_{1d}^{-1}} \\ \vdots & \ddots & \vdots \\ \mathbf{M}_{C_{d1}^{-1}} & \dots & \mathbf{M}_{C_{dd}^{-1}} \end{pmatrix}$$

- Weight-adjusted approximation for  $\mathbf{C}^{-1}$  decouples into components

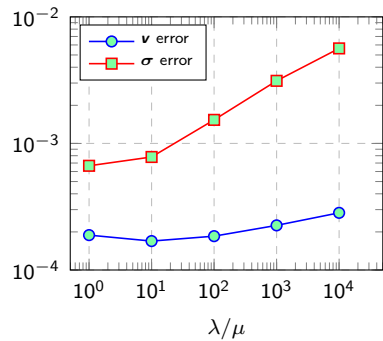
$$\mathbf{M}_{\mathbf{C}^{-1}}^{-1} \approx (\mathbf{I} \otimes \mathbf{M}^{-1}) \mathbf{M}_{\mathbf{C}} (\mathbf{I} \otimes \mathbf{M}^{-1}).$$

# Elastic wave propagation: convergence

- Convergence for harmonic oscillation, Rayleigh, Lamb, and Stoneley waves: between  $O(h^{N+1})$  and  $O(h^{N+1/2})$ .
- $\sigma$  error grows as  $\|\mathbf{C}^{-1}\| \rightarrow \infty$  (e.g. incompressible limit  $\lambda/\mu \rightarrow \infty$ ).



(a) Stoneley wave

(b)  $\|\mathbf{C}^{-1}\| \rightarrow \infty$ ,  $N = 3$ ,  $h = 1/8$ .

# Elastic wave propagation: anisotropy

No change in implementation for anisotropy - fluxes independent of  $\mathbf{C}$ .

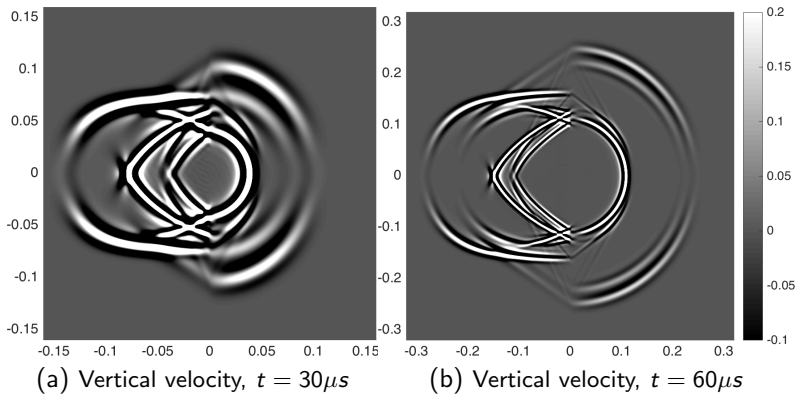


Figure: Heterogeneous media: transverse isotropy ( $x < 0$ ) and isotropy ( $x > 0$ ).

# Elastic wave propagation: 3D isotropic media

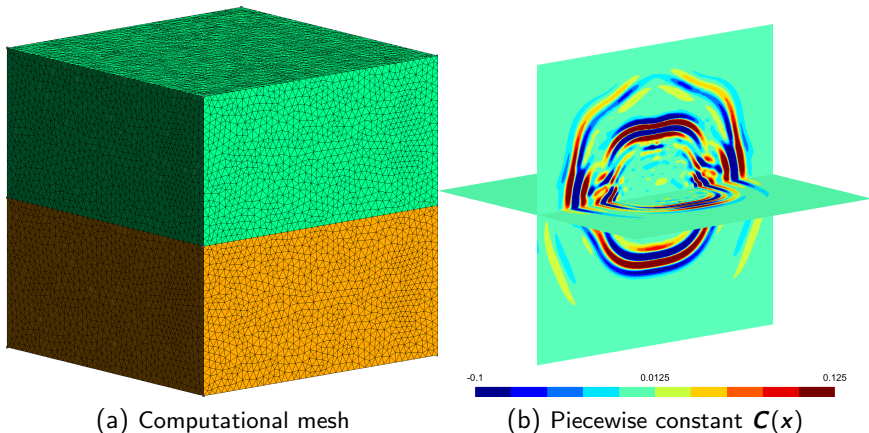


Figure:  $\text{tr}(\sigma)$  with  $\mu(x) = 1 + H(y) + \frac{1}{2} \cos(3\pi x) \cos(3\pi y) \cos(3\pi z)$ ,  $N = 5$ .

# Elastic wave propagation: 3D isotropic media

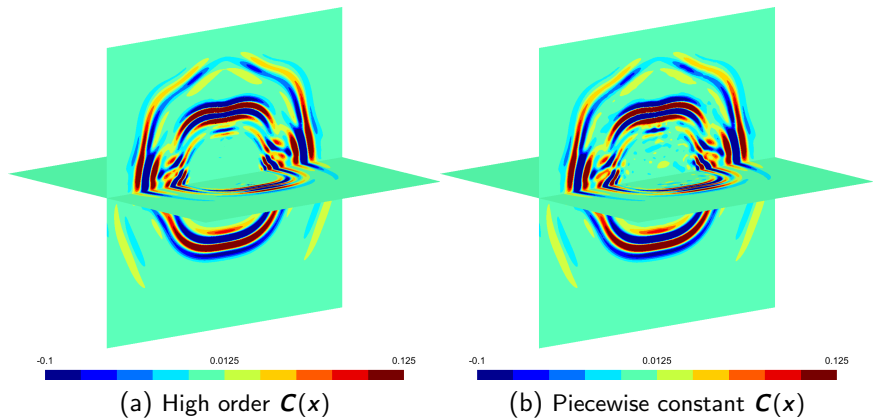


Figure:  $\text{tr}(\sigma)$  with  $\mu(x) = 1 + H(y) + \frac{1}{2} \cos(3\pi x) \cos(3\pi y) \cos(3\pi z)$ ,  $N = 5$ .

# Summary and acknowledgements

- Weight-adjusted DG (WADG): **low-storage** methods for heterogeneous media and curvilinear meshes.
- Future directions:
  - Reduce complexity of WADG using Bernstein-Bezier basis.
  - Singular weights (e.g. pyramids)?

Thanks to TOTAL E&P Research and Technology USA  
for their support of this work.

---

Chan, et al. 2016. Weight-adjusted DG methods: wave propagation in heterogeneous media (arXiv).

Chan, et al. 2016. Weight-adjusted DG methods: curvilinear meshes (arXiv).

Chan 2017. Weight-adjusted DG methods: matrix-valued weights and elastic wave prop. in heterogeneous media (arXiv).

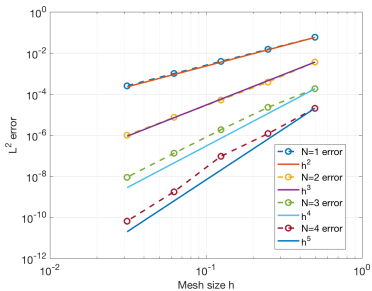
# Additional slides

# Effect of conservation on shock speeds

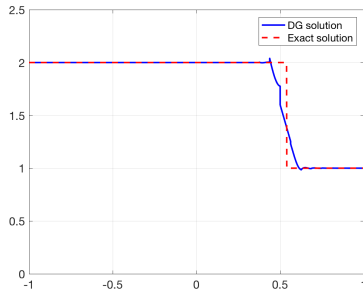
- Weighted Burgers' equation,  $w(x)$  curves characteristic lines.

$$w(x) \frac{\partial u}{\partial t} + \frac{1}{2} \frac{\partial u^2}{\partial x} = 0.$$

- WADG yields high order convergence, correct shock speed for both  $w(x)$  smooth, discontinuous (within an element).



(a) Smooth solution



(b) Shock solution

# Effect of conservation on shock speeds

- Weighted Burgers' equation,  $w(x)$  curves characteristic lines.

$$w(x) \frac{\partial u}{\partial t} + \frac{1}{2} \frac{\partial u^2}{\partial x} = 0.$$

- WADG yields high order convergence, correct shock speed for both  $w(x)$  smooth, discontinuous (within an element).

Best guess: where and what is locally conserved matters;  
non-conservation of *nonlinear flux* results in incorrect shock speeds.

# Bernstein-Bezier DG methods

- $O(N^6)$  cost in 3D ( $O(N^4)$  with tensor product) vs  $O(N^3)$  dofs.
- Sparse Bernstein-Bezier operators (( $d + 1$ ) non-zeros per row).
- Optimal  $O(N^3)$  application of derivative and lift.

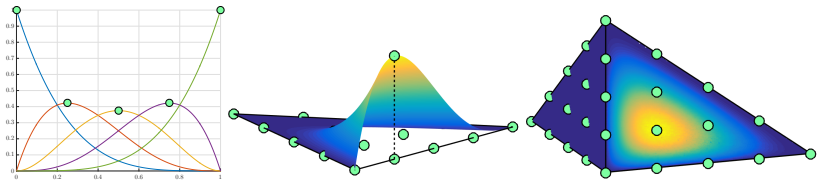
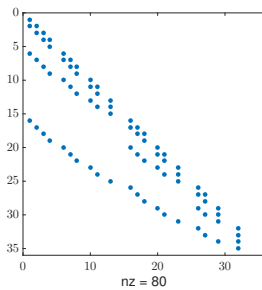


Figure: Bernstein bases in one, two, and three dimensions.

# Bernstein-Bezier DG methods

- $O(N^6)$  cost in 3D ( $O(N^4)$  with tensor product) vs  $O(N^3)$  dofs.
- Sparse Bernstein-Bezier operators (( $d + 1$ ) non-zeros per row).
- Optimal  $O(N^3)$  application of derivative and lift.



(a) Derivative operator

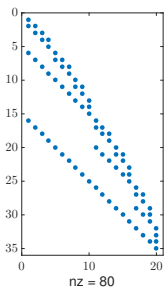
(b)  $E_{N-1}^N$ 

Figure: Sparse Bernstein derivative and degree elevation matrices.

# Bernstein-Bezier DG methods

- $O(N^6)$  cost in 3D ( $O(N^4)$  with tensor product) vs  $O(N^3)$  dofs.
- Sparse Bernstein-Bezier operators (( $d + 1$ ) non-zeros per row).
- Optimal  $O(N^3)$  application of derivative and lift.

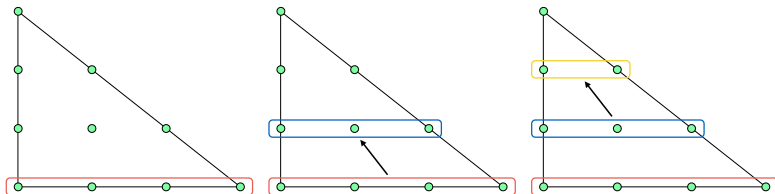


Figure: Optimal-complexity “slice-by-slice” application of Bernstein lift.

# Bernstein-Bezier DG methods

- $O(N^6)$  cost in 3D ( $O(N^4)$  with tensor product) vs  $O(N^3)$  dofs.
- Sparse Bernstein-Bezier operators (( $d + 1$ ) non-zeros per row).
- Optimal  $O(N^3)$  application of derivative and lift.

